Chapter 5

Nonlinear Dynamics of Patterns

The theory of deterministic chaos represents an important conceptual advance and offers an appropriate framework to account for experiments in confined geometry. However, it becomes rapidly inapplicable when the effective dimension of the dynamics increases, which is the case for extended systems (large aspect ratio). As already indicated, eigenmodes are then quasi-degenerate with wavevectors typically such that

$$k_{n+1} - k_n = \pi/\ell \ll k_c \,,$$

ℓ being the lateral extension (see p. 117). Many modes may be unstable close to the threshold. A large part of the interaction between them can be understood in terms of *linear* interferences accounting for spatial modulations brought to a regular uniform reference pattern (at the limit of a laterally unbounded system), e.g. parallel straight rolls for convection. At the *nonlinear* stage, focusing on the modulations directly leads one to the *envelope* formalism that gives a satisfactory account of confinement effects and defects at lowest order, a first step toward understanding *spatio-temporal chaos*.

For simplicity, we mostly limit this presentation to the case of cellular stationary instabilities. The case of dissipative waves, just briefly introduced in §5.4.4, is left to more advanced studies. We consider first, in §5.1, the determination of uniform quasi-one-dimensional structures, periodic in a single space direction. Then we generalize the theory to the case of quasi-two-dimensional patterns, with square or triangular/hexagonal plan-forms, in §5.2 and §5.3. Their most universal instability modes in terms of long wavelength perturbations are next investigated in §5.4. We conclude the chapter by §5.5 where we present some other modeling approaches that may help one analyze space-time chaotic regimes in extended systems.

5.1 Quasi-one-dimensional Cellular Structures

5.1.1 *Steady states*

Consider an instability mechanism which, like plain Rayleigh–Bénard convection, generates stationary structures locally periodic in a single space direction, say x. At the linear stage we have:

$$\mathcal{L}(\partial_x, \partial_t; R)\mathbf{V} = 0\,, \tag{5.1}$$

the solutions of which are searched for in the form:

$$\mathbf{V} = \bar{\mathbf{V}} \exp(ikx + st)\,, \tag{5.2}$$

which leads to the dispersion relation:

$$\mathcal{L}(ik, s; R) = 0\,. \tag{5.3}$$

We are particularly interested in the neighborhood of the critical conditions $R \approx R_c$, corresponding to a marginal mode $k = k_c$ for which $\mathcal{R}e(s) = \sigma = 0$. ($\mathcal{I}m(s) \equiv 0$ along a stationary instability branch.) At threshold, we have $\mathcal{L}(ik_c, 0; R_c) = 0$, so that the linear problem (5.1) has a non-trivial solution:

$$\mathbf{V}_c = \bar{\mathbf{V}}_c \exp(ik_c x) + \text{c.c.}\,, \tag{5.4}$$

where $\bar{\mathbf{V}}_c$ accounts for the structure of the critical normal mode and c.c. means 'complex conjugate'.

The nonlinear problem extending (5.1) reads:

$$\mathcal{L}(\partial_x, \partial_t; R)\mathbf{V} = \mathcal{N}(\mathbf{V}, \mathbf{V})\,, \tag{5.5}$$

where $\mathcal{N}(\mathbf{V}, \mathbf{V})$ represents the higher order terms that were neglected in the linearization procedure. The notation suggests formally quadratic nonlinearities, as in hydrodynamics. The solution is searched for as an expansion in powers of a small parameter ϵ:

$$\mathbf{V} = \epsilon\mathbf{V}_1 + \epsilon^2\mathbf{V}_2 + \epsilon^3\mathbf{V}_3 \ldots\,, \tag{5.6}$$

and, as in the calculation of the period of nonlinear oscillators (Chapter 2, especially §2.3.2.3), the control parameter is also expanded:

$$R = R_c + \epsilon R_1 + \epsilon^2 R_2 + \ldots \tag{5.7}$$

Isolating the distance to threshold in the expression of the linear part on the l.h.s. of (5.5) we can write:

$$\mathcal{L} = \mathcal{L}_c - (R - R_c)\mathcal{M}, \tag{5.8}$$

where $\mathcal{M}$ is the opposite of the formal derivative of $\mathcal{L}$ with respect to R evaluated at threshold. Inserting expansions (5.6, 5.7) into (5.5) and taking (5.8) into account, we get a series of linear problems:

$$\mathcal{L}\mathbf{V}_1 = 0 \tag{5.9}$$

$$\mathcal{L}\mathbf{V}_2 = R_1\mathcal{M}\mathbf{V}_1 + \mathcal{N}(\mathbf{V}_1, \mathbf{V}_1), \tag{5.10}$$

$$\mathcal{L}\mathbf{V}_3 = R_2\mathcal{M}\mathbf{V}_1 + R_1\mathcal{M}\mathbf{V}_2 + \mathcal{N}(\mathbf{V}_2, \mathbf{V}_1) + \mathcal{N}(\mathbf{V}_1, \mathbf{V}_2), \tag{5.11}$$

of the general form:

$$\mathcal{L}\mathbf{V}_k = \mathbf{F}_k. \tag{5.12}$$

The first problem is homogeneous. Since the critical conditions are fulfilled, it has a non-trivial solution $\mathbf{V}_1 \propto \mathbf{V}_c$. The higher order problems ($k > 1$) are all inhomogeneous and depend on the solutions computed at previous orders ($k' < k$). Unknown free quantities R_k introduced through (5.7) are fixed by the condition that the r.h.s. of (5.12) do not contain resonant terms, exactly like in the Poincaré–Lindstedt calculation, p. 55ff.

At a formal level, let the relevant scalar product[1] be denoted by $\langle ... | ... \rangle$ and the adjoint $\mathcal{L}^\dagger$ to $\mathcal{L}$ be defined by:

$$\langle \mathbf{W} | \mathcal{L}\mathbf{V} \rangle = \langle \mathbf{V} | \mathcal{L}^\dagger \mathbf{W} \rangle^*,$$

the conditions (Fredholm alternative) fixing the unknown parameters in (5.7) read:

$$\langle \tilde{\mathbf{V}} | \mathbf{F}_k \rangle = 0.$$

where $\tilde{\mathbf{V}}$ is the solution generating the kernel of $\mathcal{L}^\dagger$ ($\mathcal{L}^\dagger \tilde{\mathbf{V}} = 0$).

From (5.9) one gets $\mathbf{V}_1 \propto \mathbf{V}_c$ and when applied to (5.10), the condition for $k = 2$ yields R_1. Once this condition is fulfilled, a particular solution can be found, to which one may add an arbitrary solution of the homogeneous problem to obtain the most general solution. To fix this solution uniquely, one may ask it to be orthogonal to $\tilde{\mathbf{V}}_c$, so that it appears as a true correction to the first order solution (in the sense of the scalar product):

$$\langle \mathbf{V}_c | \mathbf{V}_2 \rangle = 0.$$

[1] See Appendix A, §A.3.2 for a reminder.

Once $\mathbf{V}_2$ is determined, it is reported in (5.11), where the sole unknown on the r.h.s. is R_2, and so on.

When $R_1 \neq 0$, one can truncate the expansion at lowest order, which gives:

$$R = R_c + \epsilon R_1 , \qquad \mathbf{V} = \epsilon \mathbf{V}_c ,$$

and, after elimination of ϵ between the two equations

$$\mathbf{V} = \frac{(R - R_c)}{R_1} \mathbf{V}_c ,$$

so that the bifurcation is in fact *two-sided*, the solution exists for both $R < R_c$ and $R > R_c$, and its amplitude varies linearly. This situation was encountered in Exercise 4.6.3, Eq. (4.59) describing what was called a *trans-critical* bifurcation where two solutions exchanged their stability. Though non-generic, this situation was shown to occur in the absence of '$A \mapsto -A$' symmetry.

In fact, it often happens that $R_1 = 0$ for symmetry reasons. This is the case of Rayleigh–Bénard convection with symmetric top/bottom boundary conditions within the Boussinesq approximation. The '$A \mapsto -A$' symmetry then results from the translation invariance by $\lambda_c/2$ in the direction perpendicular to the roll axis. When $R_1 = 0$, the lowest non-trivial truncation of the expansion is one order higher:

$$R = R_c + \epsilon^2 R_2 , \qquad \mathbf{V} = \epsilon \mathbf{V}_c + \epsilon^2 \mathbf{V}_2 ,$$

and thus, neglecting $\epsilon^2 \mathbf{V}_2$ when compared to $\epsilon \mathbf{V}_c$ for ϵ sufficiently small, we obtain:

$$\mathbf{V} \simeq \pm \sqrt{(R - R_c)/R_2}\, \mathbf{V}_c$$

The bifurcation is now *one-sided*. Bifurcated states are to be found either for $R > R_c$ when $R_2 > 0$ (*supercritical* bifurcation) or for $R < R_c$ when $R_2 < 0$ (*subcritical*).

Explicit calculation shows that Rayleigh–Bénard convection between good-conducting plates is supercritical. It is of course possible to continue the expansion and determine a more accurate solution by going to next order $k+1$ since everything is known at order k (R_{k-1}) or can be determined ($\mathbf{V}_{k-1}$) and that the compatibility condition contains only R_k as unknown.

5.1.2 *Amplitude equation*

We now turn to a variant of the same calculation that brings back a problem similar to that studied in Chapter 4, §4.1, reintroducing time in a way similar to the method of multiple scales, Chapter 2, §2.3.2.4.

We consider the emergence stationary dissipative structure and make it explicit that the bifurcation is supercritical by defining a new small parameter ε through:

$$R = R_c + \varepsilon^2 . \tag{5.13}$$

We again search the solution as an expansion:

$$\mathbf{V} = \varepsilon \mathbf{V}_1 + \varepsilon^2 \mathbf{V}_2 + \dots , \tag{5.14}$$

but we no longer assume that it is time-independent. In order to account for this new feature we introduce a *slow* time scale t_1 in addition to the natural time scale that we now denote as t_0 by setting:

$$\partial_t = \partial_{t_0} + \varepsilon^2 \partial_{t_1} . \tag{5.15}$$

The order of t_1 in ε results from the choice (5.13) and anticipates the fact that, close to the threshold, the growth rate of perturbations varies as $R - R_c$. Here, since the instability is stationary, the action of ∂_{t_0} is trivial.[2] Let us come back to (5.5) and expand also the ∂_t present in $\mathcal{L}$. With respect to system (5.9,...), in addition to the assumptions $R_1 = 0$ and $R_2 = 1$ inherent in (5.13) the first important modification enters Eq. (5.11) where a term ∂_{t_1} appears. We can thus rewrite it as:

$$\mathcal{L}\mathbf{V}_3 = \mathcal{M}\mathbf{V}_1 + \mathcal{N}(\mathbf{V}_2, \mathbf{V}_1) + \mathcal{N}(\mathbf{V}_1, \mathbf{V}_2) - \mathcal{Q}\,\partial_{t_1}\mathbf{V}_1 , \tag{5.16}$$

where $\mathcal{Q}$ is the opposite of the operator obtained by differentiating $\mathcal{L}$ with respect to ∂_t formally.

The solution at order ε reads

$$\mathbf{V}_1 = A_1 \tilde{\mathbf{V}}_c \exp(ik_c x) + \text{c.c.}$$

where A_1 is now a function of the slow variable t_1.

At order ε^2, Eq. (5.10) is left unchanged with the introduction of time. The compatibility condition that determined R_1 in the previous approach, is now trivially fulfilled by assumption. Eq. (5.10) contains non-resonant

[2] Things would be different for an oscillatory instability, in which case we would have $\partial_{t_0} = -i\omega_c$, but the approach can easily be extended owing to what we learned in Chapter 2.

terms of the form $\exp(ink_c x)$ with $n = 0$ and $n = \pm 2$ issued from the evaluation of $\mathcal{N}(A_1 \exp(ik_c x) + \text{c.c.}, A_1 \exp(ik_c x) + \text{c.c.})$. A particular solution can thus be found in the form:

$$\mathbf{V}_{2,\text{part}} = |A_1|^2 \mathbf{V}_{20} + (A_1^2 \exp(2ik_c x)\mathbf{V}_{22} + \text{c.c.}),$$

where the first subscript indicates the order in ε and the second one the harmonic generated by the nonlinear couplings. A solution of the homogeneous problem, $A_2 \bar{\mathbf{V}}_c \exp(ik_c x) + \text{c.c.}$, must be added to this particular solution in order to obtain the full solution at order ε^2.

At order ε^3, it is easily seen that Eq. (5.16) contains a certain number of resonant terms coming from the evaluation of $\mathcal{N}(\mathbf{V}_2, \mathbf{V}_1) + \mathcal{N}(\mathbf{V}_1, \mathbf{V}_2)$. Because $\mathbf{V}_{2,\text{part}}$ contains harmonics 0 and ± 2 and $\mathbf{V}_1$ harmonics ± 1, these terms contain harmonics 0 ± 1, *i.e.* ± 1, and $\pm 2 \pm 1$, producing ± 3 and ± 1. Other resonant terms come from $R_2 \mathbf{V}_1$ (with $R_2 = 1$ by definition), and $\mathcal{Q}\, \partial_{t_1} \mathbf{V}_1$. Instead of giving R_2 as in the previous approach, the compatibility condition now reads:

$$0 = A_1 \langle \tilde{\mathbf{V}} | \mathcal{M} \bar{\mathbf{V}}_c \rangle + \langle \tilde{\mathbf{V}} | \mathcal{N}(\mathbf{V}_2, \bar{\mathbf{V}}_c) + \mathcal{N}(\bar{\mathbf{V}}_c, \mathbf{V}_2) \rangle - \partial_{t_1} A_1 \langle \tilde{\mathbf{V}} | \mathcal{Q} \bar{\mathbf{V}}_c \rangle. \quad (5.17)$$

One gets easily convinced that the second term is of the form $|A_1|^2 A_1$ by counting the powers of $\exp(ik_c x)$, so that (5.17) effectively reads:

$$\tau_0 \partial_{t_1} A_1 = a A_1 - g |A_1|^2 A_1, \quad (5.18)$$

where τ_0, a, and g are constants that can be evaluated by computing the scalar products in (5.17). Returning to notations introduced in Chapter 3, especially through (3.23), p. 84, coefficient a can be identified with R_c^{-1} since the linear growth rate was defined there as $\sigma = \tau_0^{-1}(R - R_c)/R_c$.

For a stationary instability, it is easily shown that if the system is symmetrical under the change $x \mapsto -x$, then (5.18) has real coefficients since this symmetry implies symmetry under complex conjugation: $A \exp(ik_c x) \mapsto A^* \exp(-ik_c x)$. This is no longer the case for oscillatory instabilities and dissipative waves which are much more complicated in this respect, see §5.4.4 below.

The expansion can be continued. It is then observed that the freedom introduced by the R_k in (5.6) for the computation of the time-independent solutions (5.7) is now replaced by the introduction at each order of the successive amplitudes A_k. The Fredholm alternative now governs these A_k as functions of the slow time t_1.

At lowest order we have just $A = \varepsilon A_1$. Coming back to the natural time t using (5.15), observing that all terms of (5.18) are of order ε^3, we get:

$$\tau_0 \partial_t A = a(R - R_c)A - g|A|^2 A \tag{5.19}$$

called the *amplitude equation*. As announced, this result is in line with the argument developed at the beginning of Chapter 4, and especially with that leading to (4.7).

5.2 Dissipative Crystals

We now generalize the previous calculation for the case of systems that are isotropic in the (x, y) plane perpendicular to direction z singled out by the instability mechanism. The linearized problem now reads:

$$\mathcal{L}(\boldsymbol{\nabla}_\perp, \partial_t; R)\mathbf{V} = 0\,, \qquad \boldsymbol{\nabla}_\perp \equiv (\partial_x, \partial_y) \tag{5.20}$$

and, owing to the orientation degeneracy, its solution can be searched for as a superposition of plane waves with wavevectors in different directions

$$\mathbf{V}_1 = \sum_{\mathbf{k}_j} \bar{\mathbf{V}}_{\mathbf{k}_j} \exp(i\mathbf{k}_j \cdot \mathbf{x}_h) + \text{c.c.}\,, \tag{5.21}$$

with $|\mathbf{k}_j| = k_c$ for all j.

The expansion in powers of ϵ is performed as in §5.1.1 and again leads to (5.9, ...). Let us work sequentially as before. Though the equation at order ϵ^2 remains formally the same as in the one-dimensional case, the two-dimensional character of the problem implies novelty in the determination of resonant terms: nonlinearities $\mathcal{N}(\mathbf{V}_1, \mathbf{V}_1)$ that were then only able to generate the non-resonant harmonics 0 and 2, can now produce resonant combinations as shown in Figure 5.1(b).

We can now rewrite (5.10) in the form

$$\begin{aligned}\mathcal{L}\mathbf{V}_2 = R_1 \sum\nolimits_{\mathbf{k}_j} \mathcal{M}\bar{\mathbf{V}}_{\mathbf{k}_j} \exp(i\mathbf{k}_j \cdot \mathbf{x}_h) \\ + \sum\nolimits_{\mathbf{k}_{j'}, \mathbf{k}_{j''}} \mathcal{N}(\bar{\mathbf{V}}_{\mathbf{k}_{j'}}, \bar{\mathbf{V}}_{k_{j''}}) \exp(i(\mathbf{k}_{j'} + \mathbf{k}_{j''}) \cdot \mathbf{x}_h)\,,\end{aligned} \tag{5.22}$$

so that when $\mathbf{k}_{j'} + \mathbf{k}_{j''}$ falls right on the critical circle, we must compensate this term with a term in $R_1 \neq 0$ for some well chosen $\mathbf{k}_j$. In the case of formally quadratic nonlinearities, it is thus generically expected that solutions at order ϵ^2 exist in the form of regular superpositions of three wavevectors at angles $2\pi/3$ (and their opposites). Such solutions bifurcate

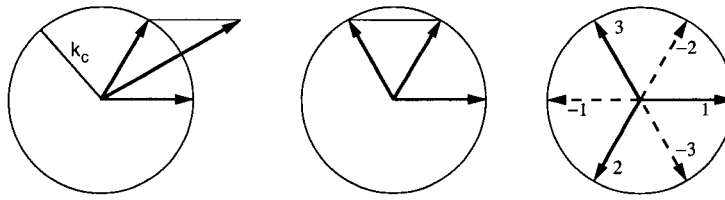

Fig. 5.1 Spatial resonance at second order: (a) Non-resonant combination $\mathbf{k} = \mathbf{k}_1 + \mathbf{k}_2$ with $|\mathbf{k}| \neq k_c$. (b) Resonant combination $\mathbf{k} = \mathbf{k}_1 + \mathbf{k}_2$ with $|\mathbf{k}| = k_c$. (c) Regular superposition of three wavevectors making a three-branch star at $2\pi/3$ forming a resonant set with their opposites (dashed arrows).

trans-critically as already shown and only special circumstances can suppress them by canceling the scalar products involving the last terms on the r.h.s. of (5.22) for symmetry reasons (e.g. the top-bottom symmetry in convection).

Let us suppose that the nonlinearities do not generate resonant terms at second order. The solution is still *a priori* made of a superposition of linear modes (5.21). So, let us consider two pairs of wavevectors $\pm\mathbf{k}_1$ and $\pm\mathbf{k}_2$ and start with:

$$\mathbf{V}_1 = \bar{\mathbf{V}}_{\mathbf{k}_1} \exp(i\mathbf{k}_1 \cdot \mathbf{x}_h) + \bar{\mathbf{V}}_{\mathbf{k}_2} \exp(i\mathbf{k}_2 \cdot \mathbf{x}_h) + \text{c.c.} \,.$$

The special solution at second order then formally reads:

$$\mathbf{V}_2 = \sum\nolimits_{\pm} \mathbf{V}^{(\pm)}_{\mathbf{k}_1,\mathbf{k}_2} \exp(i(\mathbf{k}_1 \pm \mathbf{k}_2) \cdot \mathbf{x}_h) + \text{c.c.} \,.$$

Inserting these expressions in (5.11), we obtain terms with space dependences in the form:

$$\exp(i(\mathbf{k}_{j'} + \mathbf{k}_{j''} + \mathbf{k}_{j'''}) \cdot \mathbf{x}_h), \quad \text{with} \quad \mathbf{k}_{j'}, \mathbf{k}'_{j'}, \mathbf{k}_{j'''} = \pm\mathbf{k}_1 \text{ or } \pm\mathbf{k}_2 \,,$$

so that we cannot avoid the generation of resonant terms through the relation:

$$\mathbf{k}_{j'} + \mathbf{k}_{j''} + \mathbf{k}_{j'''} = \mathbf{k} \,,$$

with $\mathbf{k}$ lying right on the critical circle, as shown in Figure 5.2.

The difficulty in the computation only comes from the fact that this relation can be fulfilled in many ways. Among all possible combinations, those involving a single pair of wavevectors are immediately identified,

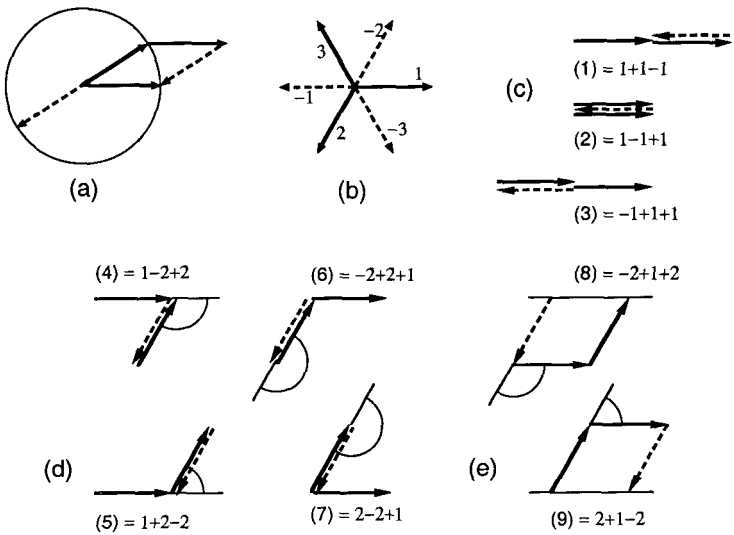

Fig. 5.2 Spatial resonance at third order: (a) An example of resonant superposition; (b) N pairs of wavevectors making an angle π/N between nearest neighbors, here with $N = 3$. (c) Combinations with a single pair of wavevectors $\pm\mathbf{k}$ (rolls). (d, e) Combinations with two pairs of wavevector forming a parallelogram, degenerate (d) or not (e).

which we already had in the quasi-one-dimensional case. But other combinations with nontrivial contribution to R_2 are readily discovered, Fig. 5.2(a), whose contributions further depend on the angles made by the wavevectors pairs in a quantitative way.

In general one is first interested in the coefficient $R_2^{(N)}$ associated to superpositions of N pairs of wavevectors forming angles of π/N between neighbors, Fig. 5.2(b). Apart from stability considerations to be examined in §5.3 below, superpositions with an arbitrary number of pairs can be considered. However, obtaining *simple* periodic patterns implies either $N = 1$ for *rolls*, $N = 2$ for *squares*, or $N = 3$ for *hexagons* as demonstrated for standard two-dimensional crystals.[3]

Superpositions with more than three regularly disposed pairs of wavevectors in general form *multi-periodic* patterns called *quasi-crystals*. The latter may degenerate into periodic *super-lattices* with large periods when certain commensurability relations are fulfilled. See Chapters 5 and 6 of [Rabinovich *et al.* (2000)]. The parallel is complete with periodic locking

[3]See, Chapter 13 of L.D. Landau & E.M. Lifshitz, *Statistical Physics* (Butterworth-Heinemann, 1980).

of quasi-periodic regimes studied in Chapter 4, §4.2.3. A natural extension of the temporal setting would suggest the existence of *chaotic crystals*.[4]

5.3 Short Term Selection of Patterns

What has just been said relates only to the existence of stationary nonlinear dissipative structures but the approach leading to the amplitude equation (5.19) for a roll pattern, characterized by a single complex amplitude A, can be reproduced for more complex patterns with superpositions of plane waves $\exp(i\mathbf{k}_j \cdot \mathbf{x}_h)$, with amplitudes A_j and their complex conjugates. Symmetry and resonance considerations (see Exercise 5.6.1) lead to phenomenological amplitude equations generalizing (5.19). Assuming formally cubic nonlinearities (or formally quadratic but such that relevant resonances at second order are killed for symmetry reasons), one obtains:

$$\tau_0 \partial_t A_j = a(R - R_c)A_j - g_0|A_j|^2 A_j - \sum\nolimits_{j'} g_{jj'}|A_{j'}|^2 A_j \qquad (5.23)$$

where coefficient g_0 and $g_{jj'}$ respectively accounts for interactions of type (c) and (d, e) displayed in Figure 5.2.

When formally quadratic interactions do not kill resonances at second order, sets of three pairs of wavevectors, $\mathbf{k}_j$, $j = 1, 2, 3$, such as in Figure 5.1(b) have to be considered with the corresponding amplitudes A_j, $j = 1, 2, 3$. The resonance condition $\mathbf{k}_1 = -\mathbf{k}_2 - \mathbf{k}_3$ then implies the presence of a term $A_2^* A_3^*$ in the equation for A_1, which leads to:

$$\tau_0 \partial_t A_1 = a(R - R_c)A_1 - \tilde{g} A_2^* A_3^* - g[|A_1|^2 + \mu(|A_2|^2 + |A_3|^2)]A_1 \qquad (5.24)$$

and two other equations obtained by circular permutation of the subscripts. Coefficients g, μ and $\tilde{g}$ in (5.24) are to be determined from a detailed nonlinear calculation or just introduced through a phenomenological argument.

Regular configurations correspond to specific fixed points of the amplitude equations (5.23) or (5.24) with $|A_j| = A$ for all j. Patterns selected by nonlinearities can be discussed from the stability of these fixed points in the strictly temporal setting of Chapters 2 and 4. The case of squares is examined in Exercise 5.6.1.

[4] A.C. Newell and Y. Pomeau, "Turbulent crystals in macroscopic systems," J. Phys. A: Math. Gen. **26** (1993) L429–L434.

5.4 Modulations and Envelope Equations

The previous analyses all referred to uniform cellular structures with wavelengths equal to the critical wavelength λ_c. By assumption, confinement effects are weak in extended geometry and thus may prove unable to control the development of such "ideal" structures. "Natural" patterns that develop are therefore usually disordered, with local vectors $\mathbf{k}$ such that $|\mathbf{k}| \approx k_c$ but with slowly variable lengths and/or orientations not everywhere perfectly aligned with the directions defining a unique underlying reference pattern. Defects can also perturb the regular ordering of the individual cells. An example from convection in a large Prandtl number fluid was displayed in Figure 3.10, p. 98. Imperfect patterns are usually called *textures*.

The problem is approached within the framework of so-called *envelope equations*, which adds a spatial meaning to the temporal dimension of the amplitude equations introduced above, thus making possible the description of slow modulations to regular patterns and universal instabilities attached to them.

The derivation again starts with a solution to the nonlinear problem as a superposition of modes but with amplitudes that can be *slowly* varying in time and space, now called *envelopes*. Through the derivation process, most specificities of the primary instability are rubbed out, so that the result is expected to bear a universal content: all patterns with the same symmetries behave in the same way. Here we restrict ourselves to a heuristic approach[5] mostly using symmetry arguments and we rest the discussion on properties of the linear *dispersion relation* in the neighborhood of the threshold as discussed earlier in Chapter 3, §3.1.6, p. 84. We consider first the case of a one-dimensional cellular instability before proceeding to several extensions.

5.4.1 *Quasi-one-dimensional cellular patterns*

At distance $r = (R - R_c)/R_c$ from threshold R_c, the growth rate of a normal mode with wavevector $k = k_c + \delta k$ is generically given by (3.26), *i.e.*:

$$\tau_0 \sigma = r - \xi_0^2 \delta k^2 . \tag{5.25}$$

[5] For technical details consult the seminal paper by A.C. Newell, "Envelope equations," Lectures in Appl. Math. **15** (1974) 157–163; or else: S. Fauve, "Pattern forming instabilities" in [Godrèche and Manneville (1998)]; A.C. Newell, Th. Passot, and J. Lega, "Order parameter equations for patterns," Annu. Rev. Fluid Mech. **25** (1993) 399–453; [Cross and Hohenberg (1993)] or else [Rabinovich *et al.* (2000)].

Slightly above threshold ($0 < r \ll 1$) the wavepackets serving to build the modulated pattern are made of unstable wavevectors (with $\sigma > 0$) in the band $k \in [k_c - \Delta k, k_c - \Delta k]$ with $\Delta k = \xi_0^{-1}\sqrt{r}$. The space modulations are thus slow when compared to variations at the scale of the wavelength λ_c ($\Delta k/k_c \ll 1$). Two time variables, t_0 and t_1, were introduced in order to obtain the amplitude equations. In the same way, two space variables are defined, a fast one and a slow one, x_0 and x_1, respectively. Like the slow time variable t_1, the slow space variable is linked to the distance to threshold r through the growth rate. From (5.25), we guess:

$$\partial_{x_1 x_1} \sim \delta k^2 \sim r\sigma \sim \partial_{t_1} .$$

A systematic expansion in powers of a small parameter ε should therefore rest on the assumptions:

$$r = \varepsilon^2 , \quad \partial_t \mapsto \partial_{t_0} + \varepsilon^2 \partial_{t_1} , \quad \partial_x \mapsto \partial_{x_0} + \varepsilon^2 \partial_{x_1} ,$$

and

$$V = \varepsilon A_1(x_1, t_1) \exp(ik_c x_0) + \text{c.c.} + \ldots$$

where the distinction between the *carrier wave* at k_c and the *modulation* is made explicit.

The translation in physical space (slow x_1) is easily obtained by formally performing an inverse Fourier transform $i\delta k \mapsto \partial_{x_1}$ which leads to

$$\tau_0 \partial_{t_1} A_1 = A_1 + \xi_0^2 \partial_{x_1 x_1} A_1 . \tag{5.26}$$

After having unfolded the space dependence we have to add the contribution of the nonlinearities previously computed and accounted for in (5.18). Back to the natural variables with $A = \varepsilon A_1$, (5.26) reads:[6]

$$\tau_0 \partial_t A = rA + \xi_0^2 \partial_{xx} A - g|A|^2 A \tag{5.27}$$

where it can be seen that each term is of order $r^{3/2}$, which is in fact the lowest significant order.

In the case of convection, Segel[7] has shown that one could account for lateral boundary effects inhibiting the instability mechanism by imposing:

$$A(x_b, t) = 0 \tag{5.28}$$

[6] As already noticed, coefficient a in (5.18) is absorbed in the definition of r.

[7] L.A. Segel, "Distant side-walls cause slow amplitude modulation of cellular convection," J. Fluid Mech. **38** (1969) 203–224.

at the position of the lateral wall x_b. In a semi-infinite medium, setting the origin at the wall, one easily determines the profile of the modulation by integrating the second order differential equation

$$\xi_0^2 \tfrac{d^2}{dx^2} A + rA - gA^3 = 0 .$$

(Since the equation is invariant under the change $A \mapsto A\exp(i\varphi)$ one can choose the phase A that makes it real.) By identification one finds

$$A = A_0 \tanh(x/\xi\sqrt{2})$$

with $A_0 = \sqrt{r/g}$ and where $\xi = \xi_0/\sqrt{r}$, often called the *coherence length*, diverges in the vicinity of the threshold.

5.4.2 *2D modulations of quasi-1D cellular patterns*

Let us now proceed to several extensions of (5.27) and first consider the case of an instability that still favors rolls but in an effective two-dimensional medium which is rotationally invariant in its plane. An argument due to Newell and Whitehead[8] shows that, x being the direction of the local wavevector and y the perpendicular direction, modulations along y are slow but faster than along x ($\partial_y \sim \mathcal{O}(r^{1/4}) \gg \partial_x \sim \mathcal{O}(r^{1/2})$ for $r \ll 1$) and that rotational invariance is accounted for by the replacement of ∂_x by $\partial_x - (i/2k_c)\partial_{yy}$ in (5.27). This substitution leads to what is known as the Newell–Whitehead–Segel (NWS) equation that reads:

$$\tau_0 \partial_t A = rA + \xi_0^2 \left[\partial_x + \frac{1}{2ik_c}\partial_{yy}\right]^2 A - g|A|^2 A , \qquad (5.29)$$

in the original variables x, y, and t, and where each term is again easily seen to be of order $r^{3/2}$.

The origin of the substitution can be understood by considering the operator $\left(\nabla_\perp^2 + k_c^2\right)^2$ from which periodic structures with space periodicity close to $\lambda_c = 2\pi/k_c$ emerge in media with rotational invariance in the (x, y) plane. Under Fourier transform, for a wavevector $\mathbf{k} = (k_c + \delta k_x)\hat{\mathbf{x}} + \delta k_y \hat{\mathbf{y}}$, at lowest significant order in $(\delta k_x, \delta k_y)$ one obtains:

$$\begin{aligned}\left[-(k_c + \delta k_x)^2 - \delta k_y^2 + k_c^2\right]^2 &\simeq \left[-2k_c \delta k_x - \delta k_y^2\right]^2 \\ &= \left[(2ik_c)(i\delta k_x) + (i\delta k_y)^2\right]^2 ,\end{aligned}$$

[8] A.C. Newell and J.A. Whitehead, "Finite bandwidth, finite amplitude convection," J. Fluid Mech. **38** (1969) 279–303.

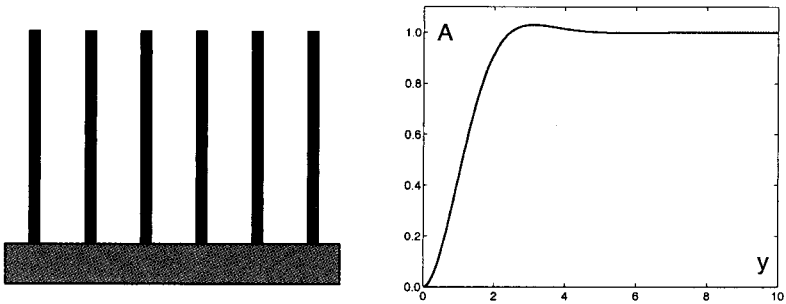

Fig. 5.3 Left: Pattern with rolls arriving perpendicular to a lateral wall. Right: Corresponding solution of (5.31).

from which the indicated replacement derives by just performing the inverse Fourier transform ($i\delta k_x \mapsto \partial_x$, $i\delta k_y \mapsto \partial_y$).

Brown and Stewartson[9] have shown that the boundary condition at a wall inhibiting the instability and perpendicular to the y direction reads:

$$A(x, y_b, t) = 0 \qquad \text{and} \qquad \partial_y A(x, y_b, t) = 0 \tag{5.30}$$

The y-dependence of the envelope in the vicinity of the lateral wall, depicted in Figure 5.3, has been obtained by numerical integration of the fourth order differential equation

$$(\xi_0^2/4{k_c}^2)\tfrac{d^4}{dy^4}A = rA - gA^3 \tag{5.31}$$

with boundary conditions (5.30) at $y = 0$ and $A \to A_0 = \sqrt{r/g}$ for $y \to \infty$. The value of the second derivative at $y = 0$ is obtained by multiplying (5.31) with $\frac{d}{dy}A$ which can be integrated. The so-obtained first integral is then evaluated at $y \to \infty$ where all derivatives of A are zero, which fixes $\frac{d^2}{dy^2}A$ at $y = 0$. Writing (5.31) as a four-dimensional first-order system, one finally obtains the solution by integrating it as an initial value problem, by means of a shooting method in which the value of the third derivative of A at $y = 0$ is the sole unknown initial condition to be adjusted so that $A(y) \to A_0$ as $y \to \infty$.

[9] S.N. Brown and K.S. Stewartson, "On finite amplitude Bénard convection in a cylindrical container," Proc. R. Soc. Lond. A **360** (1978) 455–469.

5.4.3 *Quasi-two-dimensional cellular patterns*

It is not difficult to extend the formalism to treat patterns with several pairs of wavevectors at a phenomenological level. We shall consider here only the case of a square pattern simply obtained by noticing that the x direction for one of the wavevectors is the transverse direction to the other and reciprocally. Combining results already obtained we get

$$\tau_0 \partial_t A_1 = r A_1 + \xi_0^2 \left[\partial_x + \frac{1}{2ik_c}\partial_{yy}\right]^2 A_1 - g(|A_1|^2 + \mu|A_2|^2)A_1, \quad (5.32)$$

$$\tau_0 \partial_t A_2 = r A_2 + \xi_0^2 \left[\partial_y + \frac{1}{2ik_c}\partial_{xx}\right]^2 A_2 - g(|A_2|^2 + \mu|A_1|^2)A_2. \quad (5.33)$$

When $\mu > 1$, the calculation developed in Exercise 5.6.1 shows that rolls are preferred locally.[10] Exercise 5.6.3 then shows that a system of rolls with a wavevector too far from k_c also becomes unstable against the formation of rectangles owing to the growth of a system of rolls with wavevector k_c but at right angles with it. This is the *cross-roll* instability, and the way it is shown to exist implies its *universal character*: all roll patterns in rotationally invariant media may experience it. On the other hand, owing to their local stability properties, roll systems at right angles may coexist in different but contiguous regions of space if their wavevectors are sufficiently close to k_c, forming a stationary *grain boundary*, see Figure 5.4 (left). A grain boundary parallel to the y axis is obtained by solving (5.32, 5.33) in

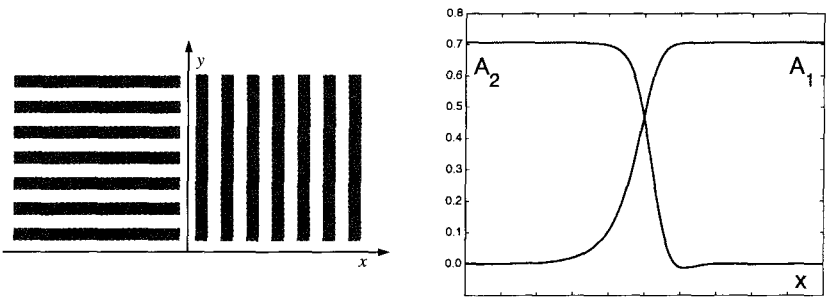

Fig. 5.4 Left: Roll system with a grain boundary. Right: Solution for the corresponding amplitudes.

[10] In essence, when $\mu < 1$, everything occurs as if $\mu = 0$, the two systems of rolls ignore each other, and grow, so that squares are obtained everywhere in space; when $\mu > 1$, they cannot but feel each other and one kills the other, at least locally.

the special case $\partial_y \boxminus 0$ which leaves one with a differential system in x. For example if both underlying wavevectors are equal to k_c, one gets:

$$0 = rA_1 + \xi_0^2 A_1'' - g(|A_1|^2 + \mu|A_2|^2)A_1,$$
$$0 = rA_2 - \frac{\xi_0^2}{4{k_c}^4} A_2'''' - g(|A_2|^2 + \mu|A_1|^2)A_2,$$

where the primes indicate differentiation with respect to x. The solution illustrated in Figure 5.4 (right) has here been rapidly and accurately obtained by searching it as the asymptotic solution of a partial differential problem in x and t using a simple numerical scheme of the kind described in Appendix B, §B.2.1. The mathematical solution can however be obtained by analytical means (matched asymptotic expansions).[11]

The envelope formalism just introduced can account for the essentials of the dynamics of *scalar* textures such as those observed in convection at large Prandtl numbers. In particular, it explains the orientation of rolls at lateral boundaries, the presence of curvature and well ordered *grains* and other *defects* such as those present in Figure 3.10, p. 98. All this follows from the fact that the NWS equation (5.29) derives from a potential in the sense of Chapter 2, §2.1.3, p. 33, *i.e.* can be written as

$$\tau_0 \partial_t A = -\frac{\delta \mathcal{G}}{\delta A^*} \tag{5.34}$$

where the right hand side is a notation representing the functional differentiation of

$$\mathcal{G}(A, A^*) = -r|A|^2 + \xi_0^2 \left| \left[\partial_x + \frac{1}{2ik_c} \partial_{yy} \right] A \right|^2 + \frac{1}{2} g |A|^4 , \tag{5.35}$$

with respect to A^*, with $g \in \mathbb{R}$, hence $\mathcal{G} \in \mathbb{R}$.

Functional differentiation in (5.34) is understood in the sense of *variation calculus*. In the change $A \mapsto A + \delta A$:

- variations of $|A|^2$ and $|A|^4$ expand as $A\,\delta A^* + A^*\delta A$ and $2|A|^2(A\,\delta A^* + A^*\delta A)$, which immediately gives the corresponding terms in (5.29) upon isolation of terms in δA^*;
- terms involving derivatives need a slightly more complicated treatment; for example, the variation of $\partial_x A\,\partial_x A^*$ gives $\partial_x A\,\partial_x \delta A^* + \partial_x \delta A\,\partial_x A^*$ but $\partial_x \delta A^*$ is not independent of δA^* so that an integration by part has to be performed to isolate the latter, which yields $-\delta A^* \partial_{xx} A$ plus boundary

[11] P. M. and Y. Pomeau, "A grain boundary in cellular structures near the onset of convection," Phil. Mag. A **48** (1983) 607–621.

terms; the other terms can be treated in the same way (two integrations by part for the terms arising from $|\partial_{yy}A|^2$) so that all the partial derivatives of (5.29) with respect to space are also recovered;

- boundary conditions (5.28, 5.30) for rolls parallel or perpendicular to the lateral boundaries may be used to cancel boundary terms arising from integrations by parts in case of a rectangular domain; otherwise contributions from the boundary term can simply be neglected when compared to bulk contributions in the general case.

The system then evolves so as to minimize the potential

$$G(t) = \int \mathcal{G}\big(A(x,y,t), A^*(x,y,t)\big)\,\mathrm{d}x\,\mathrm{d}y$$

over the domain considered since $\frac{\mathrm{d}}{\mathrm{d}t}G \leq 0$. Using the same argument as in §2.1.3, one obtains that the solution that achieves this local minimum is time independent. On this basis, selected patterns are those corresponding to stationary solutions of (5.29) at local minima of $\mathcal{G}$ (local maxima or saddles are unstable solutions). Favored textures can be found by comparing the contributions of the different causes of inhomogeneity (lateral walls, defects) to the potential increase with respect to the uniform solution.

In this context, the slow residual time dependence often observed in experiments can be attributed to higher order terms omitted in (5.29) which only holds at lowest significant order, at least in the scalar case. However, the interpretation of space-time chaos (weak turbulence) is at any rate more complex as soon as one leaves this simple framework, in particular for convection at low Prandtl numbers for which the most relevant field is no longer the temperature but the velocity.

5.4.4 *Oscillatory patterns and dissipative waves*

Up to now, we have considered only stationary instabilities. The approach in terms of envelope equations extends also in the more difficult case of oscillatory instabilities, $\omega_c \neq 0$, in particular for waves when $k_c \neq 0$. Difficulties arise from the fast time dependence, drastically destroying the relaxational property by introducing complex coefficients in the evolution equations, as in the strictly temporal setting of standard Hopf bifurcation, Chapter 4, §4.2.1.2, p. 128, and not mildly by higher order corrections as above.

Here, we just give a few results practically without derivation, inviting the reader to consult references mentioned in Note 5. As in the stationary case, the primary role is taken by the linear dispersion relation introduced in

Chapter 3, §3.1.6. Considerations about resonances developed in Chapter 4, §4.1.3, are then used to deal with nonlinearities directly written as *normal forms* relevant to the case at hand.

For an oscillatory instability with $k_c = 0$ or for a dissipative wave with $k_c \neq 0$ but in a reference frame moving at the group velocity (see p. 85), we have:

$$\tau_0 \partial_t A = (r - i\tilde{\alpha})A + \xi_0^2(1 + i\alpha)\partial_{xx}A - g(1 + i\beta)|A|^2 A\,.$$

This equation accounts for the space unfolding of the Hopf bifurcation (4.16) as derived from the dispersion relation of the corresponding instability (3.26, 3.27), p. 84. Coefficient $\tilde{\alpha}$ is the critical pulsation in units of τ_0, *i.e.* $\omega_c = \tilde{\alpha}/\tau_0$; it can be eliminated by changing to a 'rotating frame' $A(x,t) \mapsto A(x,t)\exp(-i\omega_0 t)$.

The next coefficient, α, is a measure of linear dispersion in units of the natural coherence length ξ_0^2. Finally, β is the nonlinear dispersion coefficient rescaled by g, which accounts for saturation effects by nonlinearities.

Upon further rescaling of time, length, and amplitude, one obtains the universal form of the so-called *complex Ginzburg–Landau equation* (CGL):[12]

$$\partial_t A = A + (1 + i\alpha)\partial_{xx}A - (1 + i\beta)|A|^2 A\,. \tag{5.36}$$

This formulation is not restricted to the one-dimensional case introduced here but can be extended to higher dimensions, ∂_{xx} simply being replaced by the Laplacian when the physical system is isotropic in space.

The structure of the equations governing one-dimensional waves propagating in opposite directions (complex envelopes $A_{1,2}$) can be obtained in the same way by symmetry and resonance considerations which lead to:

$$\begin{aligned}
\partial_t A_1 + v_g \partial_x A_1 &= A_1 + (1 + i\alpha)\partial_{xx}A_1 \\
&\quad - [(1 + i\beta)|A_1|^2 + (\mu' + i\mu'')|A_2|^2]A_1\,, \\
\partial_t A_2 - v_g \partial_x A_2 &= A_2 + (1 + i\alpha)\partial_{xx}A_2 \\
&\quad - [(1 + i\beta)|A_2|^2 + (\mu' + i\mu'')|A_1|^2]A_2\,,
\end{aligned}$$

through appropriate rescalings. Notice however that, since the first order partial derivative ∂_x is expected to be of order $r^{1/2}$ before rescaling, the unscaled group velocity must also be of order $r^{1/2}$ (*i.e.* small enough), to insure the consistency of the set of equations at order $r^{3/2}$.

[12] W. van Saarloos, "The complex Ginzburg–Landau equation for beginners," in [Cladis and Palffy-Muhoray (1995)].

Solutions with $A_2 = 0$ and $A_1 \neq 0$ (or the reverse) account for *propagating waves* moving to the right (or left), *i.e.* $\equiv A_1(x - vt)$ (or $\equiv A_2(x + vt)$). By contrast condition $|A_1| = |A_2|$ describes a superposition of right and left waves forming a *standing wave.* A calculation analogous to that in Exercise 5.6.1 shows that the system prefers propagating waves when $|\mu'| > 1$ (one wave "feels" the presence of the other and "kills" it) and standing waves when $|\mu'| < 1$ (each wave does not "feel" the presence of the other much and therefore "accept" cohabitation).

When propagating waves are preferred, defects similar to grain boundaries may separate homogeneous domains with opposite kinds of wave in each. These defects are called *sources* or *sinks* according to whether the waves travel away from the defect or toward it.

5.4.5 *Universal long-wavelength instabilities*

One of the interests of the envelope formalism is to offer a framework for the study of universal secondary instabilities of dissipative structures linked to the symmetry properties of patterns at the limit of a laterally unbounded system. For stationary cellular structures, two such secondary modes are the *Eckhaus instability* against local compression/expansion and the *zigzag instability* against local torsion of the rolls, as sketched in Figure 5.5.

These two universal modes are called *phase instabilities* because they relate to modulations of the position of the cells. Within the envelope approach, the solution is searched for in the form $A = |A| \exp(i\phi)$, and while the modulus $|A|$ describes the intensity of the response to the primary instability mechanism, the phase serves to specify the absolute position of the pattern in the laboratory frame. The universal instability linked to the

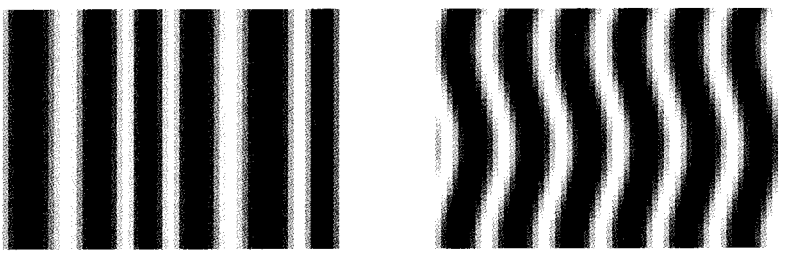

Fig. 5.5 Initial aspect of perturbation associated to the Eckhaus instability (left) and the zigzag instability (right).

amplitude is the *cross roll* instability mentioned earlier, p. 195, and further studied in Exercise 5.6.3. Contrasting with the amplitude that has a finite relaxation time, the phase is dynamically neutral as long as the solution is uniform.

A slightly irregular pattern can be described by a phase modulation which decays when the pattern is stable or gets amplified when it is unstable. Typically, at least for scalar dissipative structures, the phase of the envelope is governed by a diffusion equation:

$$\partial_t \phi = D_{\|} \partial_{xx} \phi + D_{\perp} \partial_{yy} \phi , \tag{5.37}$$

where $D_{\|}$ and $D_{\perp}$ are diffusion coefficients along the wavevector of the structure, or perpendicular to it. As long as these coefficients are both positive, the phase perturbation relaxes and the roll pattern is stable against (infinitesimal) phase perturbations. The instability is observed when one of these coefficients changes its sign. The Eckhaus instability corresponds to $D_{\|}$ becoming negative, and the zigzag when it is $D_{\perp}$.

The phase diffusion coefficients depend on the wavelength of the underlying pattern. Exercise 5.6.2 is a first approach to the Eckhaus instability resting on (5.27), the zigzag instability would be studied in the same way using (5.29). The result is generally presented as a stability diagram in the parameter plane $(\delta k, r)$ where δk measures how the wavevector of the underlying pattern departs from the critical wavevector and r is the control parameter. Figure 5.6 displays the results at lowest significant order.

The Eckhaus instability is a *side-band instability* that develops "far from" k_c and close to the marginal stability curve, in a region where the instability mechanism is not very efficient and the amplitude of the solution, $A_0 = \sqrt{(r - \xi_0^2 \delta k^2)/g}$, is small. "Preferring" a solution with a more optimal wavevector, the system amplifies the phase modulation by compressing certain regions and expanding others (Fig. 5.5, left). Supposing for example that the initial wavelength is too short, expanded regions will have a more favorable local wavevector while in compressed regions the local wavelength will be even shorter. The primary mode completely disappears at the location of the most compressed places since the amplitude of the primary mode drops to zero at the marginal stability curve. The pattern then loses a pair of rolls at such places and the wavelength further relaxes toward an increased more optimal value. If the obtained wavevector is still in the unstable domain, the process repeats. If not, it stops and the system evolves through diffusive relaxation toward a uniform pattern with a wavelength inside the stable domain.

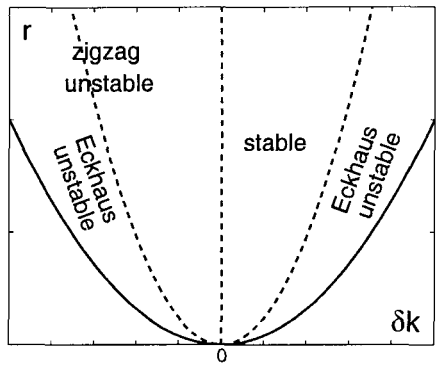

Fig. 5.6 Stability diagram of roll patterns against universal phase modes of compression/expansion (Eckhaus) and torsion (zigzag). As obtained from equation (5.29) valid at lowest order, the marginal stability curve is given by $r = \xi_0^2 \delta k^2$. Rolls are unstable against the Eckhaus mode in the region $\xi_0^2 \delta k^2 < r < 3\xi_0^3 \delta k^2$. The zigzag instability domain is for $\delta k < 0$. Stable rolls have wavevectors in the domain $0 < \delta k$, $r > 3\xi_0^3 \delta k^2$.

The zigzag instability sets in when $\delta k < 0$, *i.e.* for wavelengths larger than critical. This can also be easily interpreted by noticing (Fig. 5.5, right) that, when measured perpendicularly to the local axis of the rolls, the wavelength is shorter than that measured along the x axis by a factor equal to the cosine of the angle between the local periodicity direction and the x axis. The instability again develops so as to make the (too long) initial wavelength shorter and thus closer to the critical value. By contrast with the case of the Eckhaus instability which changes the number of rolls, the zigzag instability saturates as it amplifies. The process ends in wide regularly spaced domains of 'zig' and 'zag' straight rolls connected by barrow bands of strong bending.

Up to now, we have only considered the initial development of these universal phase instabilities and just sketched the ultimate fate of the unstable state. Analytically, one can go a little further and complete the phase diffusion equation (5.37) by appropriate nonlinearities. In this context, let us mention the *Kuramoto–Sivashinsky equation*[13] (KS) to be used in the numerical experiments described at the end of Appendix B. This equation describes the dynamics of the phase of nearly uniform solutions to the complex Ginzburg–Landau equation (5.36) in a narrow neighborhood of the threshold of the *Benjamin–Feir* instability.

[13]Y. Kuramoto, "Phase dynamics of weakly unstable periodic structures," Prog. Theor. Phys. **71** (1984) 1182–1196.

On general grounds this instability, which closely corresponds to the Eckhaus instability of one-dimensional stationary patterns, develops when the phase diffusion coefficient $D = 1 + \alpha\beta$ becomes negative (*Newell's criterion*, see Note 5. By symmetry considerations one can check that the equation governing the phase, at most quadratic in ϕ and up to order four in ∂_x, reads:

$$\partial_t\phi = D\partial_{xx}\phi - K\partial_{xxxx}\phi + g_0(\partial_x\phi)^2 + g_1(\partial_x\phi)(\partial_{xxx}\phi) + g_2(\partial_{xx}\phi)^2 + g_3(\partial_x\phi)^2(\partial_{xx}\phi)\,, \tag{5.38}$$

where each coefficient can be derived from those in (5.36). In addition to $D = 1 + \alpha\beta$, one gets[14] $K = \frac{1}{2}\alpha^2(1+\beta^2) > 0$, $g_0 = \beta - \alpha$, $g_1 = 2g_2 = \alpha g_3 = -2\alpha(1+\beta^2)$.

In practice, for $D \approx 0$ but negative, the order of magnitude of the space gradient is fixed by the competition between the two linear terms and all nonlinear terms except the first can be neglected. After appropriate rescalings, Equation (5.38) can be reduced to the KS equation which reads in universal form:[15]

$$\partial_t\phi + \partial_{xx}\phi + \partial_{xxxx}\phi + \tfrac{1}{2}(\partial_x\phi)^2 = 0 \tag{5.39}$$

or, after differentiating it with respect to x and setting $\psi = \partial_x\phi$:

$$\partial_t\psi + \psi\partial_x\psi + \partial_{xx}\psi + \partial_{xxxx}\psi = 0\,. \tag{5.40}$$

The nonlinearity $\psi\partial_x\psi$ present in this last expression is reminiscent of the advection term of hydrodynamics. It already appeared in the *Burgers* equation (Chapter 1, Exercise 1.5.3) producing shocks (Exercise 5.6.4, part 1) and the *Korteweg–de Vries* equation producing solitons (Chapter 2, Exercise 2.5.6). The KS equation in one or the other form, (5.39) or (5.40) is a particularly simple model of *phase turbulence*.[16]

As long as D remains small, the modulus of the envelope is enslaved to the phase gradient, stays close to its nominal value A_0, and therefore remains bounded away from zero. This is no longer the case when the phase instability is more intense. The field $|A|$ then revolts and recovers a

[14] J. Lega, *Défauts topologiques associés à la brisure d'invariance de translation dans le temps*, PhD Dissertation, Nice University, 1989 (in French).

[15] The equation also appears in problems of front propagation as shown by G.I. Sivashinsky, "On self-turbulization of a laminar flame," Acta Astronautica **6** (1979) 569–591; hence the joint names for the equation.

[16] For a brief review with references, see: H. Chaté and P. M., "Phase turbulence," in [Tabeling and Cardoso (1994)].

dynamics of its own. It then explores a larger range of values that extends down to zero. At places where $|A| = 0$, the phase is no longer defined and phase defects nucleate, with 2π-jumps of ϕ. The CGL equation then enters new regimes whose precise nature depends on the value of α and β in (5.36) and the space dimension. Strong space-time chaos called *defect turbulence* then sets in. In two dimensions, it is characterized by the permanent birth of defects in pairs, that further dissociate and move around before merging.[17]

The theory of the transition to chaos is rooted in the idea of dimensional reduction leading to effective dynamical systems in terms of ordinary differential equations. To summarize this section, one can say that the envelope formalism is the required adaptation of this idea when confinement effects are too weak to legitimate the approach in terms of isolated modes and corresponding discrete amplitudes. Pattern selection strictly relies on this reduction for uniform solutions.

Defects and universal secondary instabilities involve modulations to some ideal reference situation. As long as the system remains sufficiently close to a stable regularly ordered pattern, the relevant instability modes relates to the phase of envelope and a supplementary reduction is possible by adiabatic elimination of the envelope modulus. Localized defects also play a role, either because they are present in the initial conditions (when the pattern emerges) or as the result of secondary instabilities that do not saturate. Sometimes tools borrowed from the theory of dynamical systems can still be used, e.g. to determine special solutions to the envelope equations.

It should also be noticed that, while the envelope formalism can be made rigorous within the framework of multiple scale methods, an interesting alternative is the derivation of generic models by phenomenological arguments resting on resonance and symmetry considerations. Further, the numerical simulation of such models has proved crucial to the understanding of space-time chaos. Such simulations usually do not require considerable investment and the reader is encouraged to practice them using the simple numerical methods presented in Appendix B, in order to get a personal intuition of the problem while taking advantage of the published material listed in, e.g. [Rabinovich *et al.* (2000)] or to be found on the Internet.

[17] P. Coullet, L. Gil, J. Lega, "Defect-mediated turbulence," Phys. Rev. Lett. **62** (1989) 1619–1622. A complete phase diagram is given in the one-dimensional case by H. Chaté, "Disordered regimes of the one-dimensional complex Ginzburg–Landau equation," in [Cladis and Palffy-Muhoray (1995)].

5.5 What Lies Beyond?

Before closing this chapter, let us point out the interest of fully analogical approaches to the modeling of extended systems, useful when the minimum space-time coherence necessary to apply the envelope formalism is absent from the system. As a matter of fact, when the space-time coherence is limited, there is some advantage to consider the continuous system as an aggregate of subsystems coupled to each other. The local dynamics is accounted for at the scale of the subsystem while the space extension arises through the coupling between the subsystems usually arranged at the node of a lattice.

A system can thus be discretized at several levels. At first, one can just discretize the physical space and get lattices of differential systems, e.g. lattices of Hopf oscillators or Lorenz systems. These systems are then coupled by some rule. For example, nearest-neighbor diffusive coupling of identical Hopf oscillators in one dimension would yield

$$\frac{\mathrm{d}}{\mathrm{d}t} Z_n = (r - i\omega) Z_n - g|Z_n|^2 Z_n + D(Z_{n+1} - 2Z_n + Z_{n-1}),$$

where subscript n indicates the space position of an individual oscillator and the discrete version of the diffusion operator, here $D\partial_{xx}$ is easily recognized.

Next step, time can also be discretized, which gives *coupled map lattices*. Time and space being indicated by superscript k and subscript n, respectively, in one dimension and again for diffusive coupling, one will start with

$$\mathbf{X}_n^{k+1} = (1 - 2D)\boldsymbol{\mathcal{F}}\left(\mathbf{X}_n^k\right) + D\left[\boldsymbol{\mathcal{F}}\left(\mathbf{X}_{n+1}^k\right) + \boldsymbol{\mathcal{F}}\left(\mathbf{X}_{n-1}^k\right)\right],$$

which is preferable to the seemingly more straightforward formulation:

$$\mathbf{X}_n^{k+1} = \boldsymbol{\mathcal{F}}\left(\mathbf{X}_n^k\right) + D\left[\mathbf{X}_{n+1}^k - 2\mathbf{X}_n^k + \mathbf{X}_{n-1}^k\right],$$

since it is immediately checked that the latter may not preserve the invariant domain of each subsystem while the former does (if $\mathbf{X} \in \mathcal{D}$ implies $\boldsymbol{\mathcal{F}}(\mathbf{X}) \in \mathcal{D}$, then $\mathbf{X}_n^k \in \mathcal{D}$ implies $\mathbf{X}_n^{k+1} \in \mathcal{D}$ for all n). The appropriateness of the model relies entirely on the skill of the modeler while choosing the local map and the type of coupling.[18]

Up to now, the local phase space was still a continuous set. One can make a last step by considering *cellular automata* where each subsystem

[18] See for example [Kaneko (1993)] and for a specific application H. Chaté and P. M., "Spatiotemporal intermittency" in [Tabeling and Cardoso (1994)].

can be in one of a finite set of states. Boolean automata have states labelled by bits 0 and 1, with evolution rules functions of the configuration of the neighborhood of each cell. Such systems can already have complicated dynamics in spite of very simple definitions [Wolfram (1986)].

Lattice gas automata are automata specially adapted to hydrodynamics. They describe fluids at the level of individual molecules but governed by simplified evolution rules. "Living" at the nodes of a regular lattice, the molecules can be in one of a discrete set of motion state (speed and orientation), jump from node to node and change their state of motion when they meet at some given node according to rules given in collision tables. At first, when massively parallel computers began to appear, they were presented as an alternative to the direct numerical simulation of hydrodynamics equations. Nowadays, they are rather considered as useful models when the local dynamics is rich or complicated (chemical reactions), or when the boundaries have a complex topology or special physical properties (surface catalysis). An interesting review of lattice gas automata as applied to complex hydrodynamics is [Rothman and Zaleski (1997)].

The present chapter was mostly devoted to stationary patterns in weakly confined systems, with only a few words about waves. The latter will be central to the study of open flow instabilities in the next chapter.

5.6 Exercises

5.6.1 *Pattern selection*

Consider patterns described by superpositions of plane waves:

$$V = \sum_j \tfrac{1}{2}[A_j \exp(i\mathbf{k}_j \cdot \mathbf{x}_h) + \text{c.c.}]\,,$$

namely, rolls with a single pair of wavevectors and squares with two pairs at right angles. The wavelength of the participating modes is $\lambda_c = 2\pi/k_c$.
1) Show that translational invariance along wavevector $\mathbf{k}_j = k_c\hat{\mathbf{x}}_j$ (unit vector $\hat{\mathbf{x}}_j$), $x_j \mapsto x_j + {x_j}^{(0)}$, $j = 1, 2$, implies a (gauge) invariance for the corresponding complex amplitude $A_j \mapsto A_j \exp(i{\phi_j}^{(0)})$.

Taking these symmetries into account, show that the supercritical bifurcation towards a uniform pattern is governed at lowest order by

$$\tfrac{\mathrm{d}}{\mathrm{d}t}A_1 = rA_1 - g_{11}|A_1|^2A_1 - g_{12}|A_2|^2A_1 \qquad (5.41)$$

$$\tfrac{\mathrm{d}}{\mathrm{d}t}A_2 = rA_2 - g_{22}|A_2|^2A_2 - g_{21}|A_1|^2A_2 \qquad (5.42)$$

with $g_{ij} \in \mathbb{R}$. Use the rotational invariance to reduce the number of interaction coefficients to g (self-interaction) and $g' = \mu g$ (cross-interaction). Show that g can be eliminated by appropriate rescaling of A_1 and A_2.

2) Determine the potential $G(A_1, A_1^*, A_2, A_2^*)$ from which (5.41, 5.42) derives in the sense of (5.34), here simply

$$\frac{\mathrm{d}}{\mathrm{d}t} A_j = -\partial G / \partial A_j^* .$$

and conclude that permanent regimes are time-independent.

3) Find all fixed points (A_{1*}, A_{2*}) of system (5.41, 5.42) and, apart from the trivial solution, give their explicit expression and physical significance (take advantage of the gauge invariance to specify the phase of the envelopes so as to have real amplitudes).

4) Compute the value of the potential and study its curvature at the different fixed points to guess their stability properties. Then perform the explicit stability analysis by inserting $A_j = A_{j*} + a_j$ in the system and linearizing. Even though the A_{j*} are real quantities, the most general perturbations are not, thus take $a_j = u_j + iv_j$. Show that the fourth order linear system obtained splits into two subsystems, producing two neutral modes (explain their origin) and two non-trivial modes that can be stable or unstable, according to the value of μ and the considered fixed point. Use the result to interpret phase portraits displayed in Figure 5.7. What happens when $\mu = 1$?

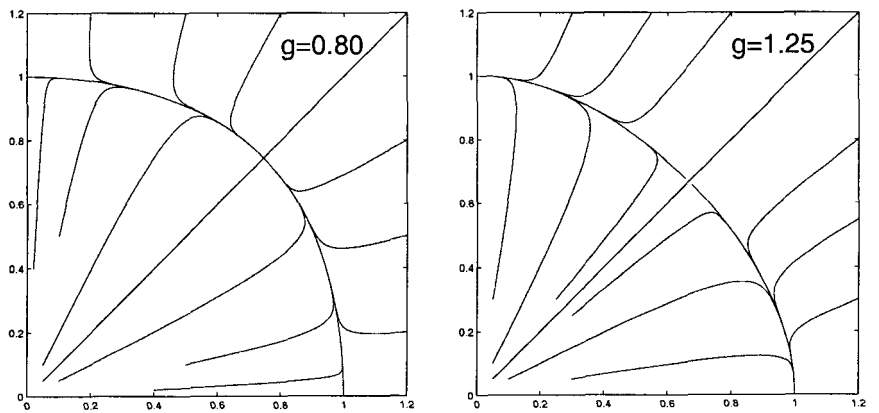

Fig. 5.7 Phase portrait of system (5.41, 5.42) for $\mu = 0.80$ (left) and $\mu = 1.25$ (right).

5.6.2 *Eckhaus instability*

Consider a roll pattern described by an envelope evolving according to:

$$\partial_t A = rA + \partial_{xx} A - |A|^2 A\,. \tag{5.43}$$

The Eckhaus instability relates to the phase ϕ of the complex field A.

1) Determine amplitude $\tilde{A}^{(0)}$ of a *phase-winding* solution corresponding to uniform rolls with wavevector $k = k_c + \delta k$, $A(x,t) = \tilde{A}^{(0)} \exp(i\,\delta k\, x)$.

The stability of this solution against long wavelength perturbations (phase modes) is studied by assuming that the prefactor of $\exp(i\,\delta k\, x)$ can be a function of space and time. From (5.43), derive the equation governing $\tilde{A}(x,t)$ defined through $A(x,t) = \tilde{A}(x,t)\exp(i\,\delta k\, x)$.

2) Insert $\tilde{A}(x,t) = \tilde{A}^{(0)} + a(x,t)$ in this new equation, and show that the linearized equations governing the real and imaginary parts of $a(x,t) = u(x,t) + iv(x,t)$ read:

$$\begin{aligned}
\partial_t u &= -2(r - \delta k^2)u + \partial_{xx} u - 2\delta k \partial_x v\,,\\
\partial_t v &= 2\delta k \partial_x u + \partial_{xx} v\,.
\end{aligned}$$

Derive the dispersion relation for Fourier normal modes with growth rate s and wavevector q taken in the form $u = \bar{u}\exp(s\,t)\cos(q\,x)$ and $v = \bar{v}\exp(s\,t)\sin(q\,x)$.

3) Show that the roots are real and that the phase-winding solution is unstable when

$$2(r - 3\delta k^2) + q^2 \leq 0\,,$$

derive from this that the instability occurs first for $q \to 0$ (long wavelength) and recover the result displayed in Figure 5.6.

5.6.3 *Cross roll instability*

In the conditions of Exercise 5.6.1, assume $\mu > 1$ (rolls preferred to squares), consider a phase winding solution with $k_x = k_c + \delta k$, and study its stability against rolls at right angles with $k_y = k_c$.

From (5.32, 5.33), show that:

$$\begin{aligned}
\tfrac{\mathrm{d}}{\mathrm{d}t} A_1 &= rA_1 + \partial_{xx} A_1 - g(|A_1|^2 + \mu|A_2|^2)A_1\,,\\
\tfrac{\mathrm{d}}{\mathrm{d}t} A_2 &= rA_2 - g(|A_2|^2 + \mu|A_1|^2)A_2\,,
\end{aligned}$$

is an appropriate starting point.

Show that the condition for instability has the same form as the Eckhaus condition but with a different prefactor to be determined. Compute the value of μ that makes the cross-roll instability more dangerous than the Eckhaus instability and interpret the limit $\mu \to 1$.

5.6.4 *Dynamical systems and nonlinear waves*

5.6.4.1 *The Burgers equation*

Consider the Burgers equation:

$$\partial_t v + v\partial_x v = \nu \partial_{xx} v \,.$$

1) Show that it is invariant through a Galilean change of frame (*i.e.* that the equation for $\tilde{v}(\tilde{x}, t)$ with $\tilde{x} = x - Vt$ and $\tilde{v} = v - V$ is the same as that governing $v(x, t)$). (The corresponding symmetry of the NS equation is discussed in Note 9, p. 239.)

2) Derive the differential equation governing a solution that propagates at speed V without deformation ($\tilde{x} = x - Vt$ is the sole independent variable) and integrate it once with respect to x. Consider a solution such that $v_\pm$ for $\tilde{x} \to \pm\infty$, derive its speed V from the first integral just obtained, and derive the analytical shape of the corresponding solution.
[Solution: a hyperbolic tangent.]

5.6.4.2 *Kuramoto-Sivashinsky equation*

Consider variant (5.40) of the KS equation:

$$\partial_t v + v\partial_x v + \partial_{xx} v + \partial_{xxxx} v = 0 \,.$$

1) Derive the linear dispersion relation governing infinitesimal perturbations $\delta v = \bar{\delta v} \exp(st + iqx)$ to the trivial solution $v \equiv 0$. Show the instability of those belonging to a range of q to be determined.

2) Write down the ordinary differential equation in $\tilde{x} = x - Vt$ governing a solitary wave solution propagating without deformation in a frame moving at speed V and derive a first integral. By identification, find a solution in the form

$$\tilde{v} = \alpha \tanh(\kappa \tilde{x}) + \beta \tanh^3(\kappa \tilde{x}) \,.$$

and compare the value of κ with the wavevector $q_{\max}$ of the perturbation with maximum growth rate $s_{\max}$.

5.6.4.3 *Flow down an inclined plane*

The Benney equation is a partial differential equation governing the long wavelength perturbations to a fluid film of uniform thickness flowing down an inclined plane. After appropriate rescalings of length, time, and film thickness, one obtains[19]

$$\partial_t h + \tfrac{2}{3}\partial_x \left[h^3 + \left(\alpha h^6 - h^3\right)\partial_x h + h^3 \partial_{xxx} h\right] = 0$$

where α is the control parameter.

1) Derive the linearized equation governing infinitesimal perturbations to a time-independent uniform solution $h = h_0$. Show that solution $h \equiv h_0 = 1$ is linearly unstable for $\alpha > \alpha_c = 1$.

2) A hydraulic jump is a solution such that $h \to 1$ for $x \to -\infty$ and $h \to h_\infty$ for $x \to +\infty$. A solitary wave precisely corresponds to $h_\infty = 1$. Write down the ordinary differential equation in $\tilde{x} = x - Vt$ governing a solution that propagates without deformation in a frame moving at speed V, integrate this equation to find a first integral and determine the value K of this first integral as a function of c when $x \to -\infty$. Then derive the relation between V and $h_\infty < 1$.

[19] See: A. Pumir, P. M., Y. Pomeau, "On solitary waves running down an inclined plane," J. Fluid Mech. **135** (1983) 27–50, and cited references.